Title: Inhibition of KIF20A by BKS0349 reduces endometriotic lesions in a xenograft mouse model

Running title: BKS0349 reduces endometriotic lesions

Authors: Ferrero H[1,2,†,*], Corachán A[1,3,†], Quiñonero A[1], Bougeret C[4], Pouletty P[4], Pellicer A[1,3], Domínguez F[1,5].

†Ferrero H. and Corachán A. should be considered as joint first authors

[1]Fundación Instituto Valenciano de Infertilidad (FIVI), Instituto Universitario IVI (IUIVI), Valencia, 46026, Spain; [2]INCLIVA Biomedical Research Institute, Valencia, 46010, Spain; [3]Department of Pediatrics, Obstetrics and Gynecology, University of Valencia, Valencia, 46010, Spain; [4]Biokinesis SAS, Paris, 75008, France; [5]Health Research Institute la Fe, Valencia, 46026, Spain

***Correspondence address:** Hortensia Ferrero Chafer, Fundación IVI/INCLIVA, Avenida Fernando Abril Martorell 106, Torre A, Planta 1ª, 46026, Valencia. E-mail: hortensia.ferrero@ivirma.com

Abstract

Several studies have suggested a possible etiological association between ovarian endometriosis and ovarian cancer. Evidence has shown that *KIF20A* overexpression might confer a malignant phenotype to ovarian tumors by promoting proliferation and inhibiting apoptosis. However, no data about the role of *KIF20A* in endometriosis have been described. In this study human endometrium (n=4) was transfected by mCherry adenovirus and intraperitoneally implanted in mice. Subsequently, mice were divided in three groups (n=8/group) that were treated with Vehicle, BKS0349 (KIF20A-antagonist) or Cabergoline (dopamine receptor agonist) for 21 days. mCherry-labeled endometriotic lesions were monitored over time using the IVIS-Imaging System. Mice were sacrificed 72h after the last administration, proliferation was evaluated by immunohistochemistry and apoptosis by TUNEL. *CCND1* gene expression (G1 phase-related gene) was measured by qRT-PCR. A significant reduction in mCherry-fluorescent signal was observed in the BKS0349 group after treatment ended (D24) compared to D0 (p-value=0.0313). Moreover, mCherry-signal on D24 showed a significant decrease in the BKS0349 group compared to controls (p-value=0.0303), along with significant size reduction of endometriotic lesions observed in BKS0349 group compared to control on D24 (p-value=0.0006). Functional studies showed a significant reduction in proliferating cells in BKS0349-treated group compared to controls (p-value=0.0082). In addition, *CCND1* expression was decreased in BKS0349 group compared to control (p-value=0.049) at D24 and a significant increase in apoptotic cells among endometriotic lesions in BKS0349-treated mice was observed compared to control (p-value=0.0317). Based on these findings, we concluded that BKS0349 induces apoptosis and inhibits cell proliferation, reducing endometriotic lesion size and suggesting KIF20A inhibition by BKS0349 as a novel therapeutic treatment for endometriosis.

Keywords: KIF20A, endometriosis, cell proliferation, cell cycle, apoptosis

Introduction

Endometriosis is an estrogen-dependent gynecologic disorder characterized by the presence of endometrial tissue outside the uterus, most commonly in the ovaries and peritoneal cavity (Kennedy *et al.*, 2005). The nature of this disease is heterogeneous and includes different anatomical entities such as ovarian, peritoneal, and deep infiltrating endometriosis, causing a range of severity of pelvic pain, dysmenorrhea, dyspareunia, painful defecation, and/or infertility (Practice Committee of the American Society for Reproductive Medicine, 2004). While endometriosis is diagnosed in 6–10% of all women, an estimated 35–50% of infertile women are affected by this disease (Giudice and Kao, 2004).

Although endometriosis is a chronic and recurrent condition, surgical removal of ectopic endometrial lesions has been the primary therapeutic approach for more than a century. However, this treatment approach provides only temporary relief as recurrence of endometriotic lesions can occur in up to 75% of cases within two years of corrective surgery (Giudice, 2010). Hormone treatments have also been used to reduce ectopic endometrial lesions; however, these treatments often fail to provide long-term relief and result in a hypoestrogenic state linked to secondary effects like osteoporosis and pseudo-menopause (Küpker *et al.*, 2002), limiting the therapy duration. Therefore, there is a need for an efficient, non-surgical treatment that reduces ectopic endometrial lesions with lasting impact and minimal side effects.

Although endometriosis is a benign condition, it shares some characteristics of malignancy, such as local and distant dissemination, cell invasion, and damage of adjacent tissue (Sayasneh *et al.*, 2011; Zafrakas *et al.*, 2014). Ovarian endometriotic cysts have recently been suggested as the origin of ovarian clear cell carcinoma (CCC) and ovarian endometrioid cancer (EC) types, implicating a possible etiological association between endometriosis and ovarian cancer (Anglesio and Yong, 2017; Barreta *et al.*, 2019). In this regard, an study about the frequency of endometriosis-associated ovarian carcinoma described that a 35% of CCC and 27% of EC have origin from endometriosis (Somigliana *et al.*, 2006; Kajiyama *et al.*, 2019). Indeed, endometriotic lesions can undergo immunohistological and molecular alterations similar to

those observed in ovarian tumors, suggesting that endometriosis may be an intermediate step in neoplastic progression (Komiyama *et al.*, 2018).

KIF20A is an overexpressed gene in most ovarian carcinoma tissues and its expression is correlated with tumor progression, suggesting that *KIF20A* may be useful as an independent prognostic biomarker in ovarian carcinoma (Li *et al.*, 2018). KIF20A, also known as RAM6KIFL/MKLP2, is a microtubule-associated motor protein in the kinesin-6 superfamily localized in the Golgi apparatus where is involved in the dynamics of this organelle and consequently, implicated in the formation of the mitotic spindle and chromosome partitioning (Verhey and Hammond, 2009), cell adhesion, spreading, migration, proliferation, and intracellular transport (Echard *et al.*, 1998; Li *et al.*, 2018). KIF20A overexpression is correlated with progression of several human malignant tumors including bladder, breast, gastric, pancreatic, small cell lung, and hepatocellular carcinoma (Kikuchi *et al.*, 2003; Claerhout *et al.*, 2011; Imai *et al.*, 2011; Ho *et al.*, 2012; Shi *et al.*, 2016; Zhao *et al.*, 2018). These findings suggest that KIF20A is involved in tumor progression by promoting cell proliferation, angiogenesis, invasion, metastasis, and autophagy and inhibiting apoptosis. Thus, KIF20A is used as an indicator of prognosis for tumors in clinical practice (Zhao *et al.*, 2018) due to its important role in cell cycle regulation.

Cell cycle is one of the molecular functions involved in cancer development, a dysregulation of this function can lead to an increased cell proliferation and consequently, tumor progression. In this regard, KIF20A affects cell proliferation by modulating the G1/S phase transition, which is a major checkpoint in cell cycle progression, and promotes apoptosis (Wang *et al.*, 2017; Zhao *et al.*, 2018). Recent evidence indicates that KIF20A inhibition can suppress the cell cycle transition from the G0/G1 phase to the S phase, causing cell cycle arrest and consequently, inhibition of cell proliferation. This implicates KIF20A as an anti-cancer drug target. Paprotrain (PAssenger PROteins TRAnsport Inhibitor; BKS0101) is reported to suppress cytokinesis by specifically inhibiting KIF20A (also known as MKLP2 inhibitor) (Tcherniuk *et al.*, 2010; Labrière *et al.*, 2016). In this regard, Paprotrain has been described as a potent inhibitor of

KIF20A in HL60 (Human myeloid leukemia cell line), leading to multinuclearity of these cells and suppressing cell growth (Morita *et al.*, 2018), suggesting KIF20A inhibition could be one of the therapeutic targets of acute leukemia. In addition, Paprotrain may be a useful tool not only for the study of KIF20A function in cytokinesis, but also to validate cytokinesis-specific kinesins as potential targets for drug development in cancer chemotherapy. Accordingly, the *in vitro* inhibition of KIF20A in cancer cells by Paprotrain or BKS0349, a new KIF20A-specific inhibitor derived from Paprotrain with higher affinity (unpublished data), showed an inhibition from the Golgi complex and a delay in vesicle transport to the plasma membrane. These findings suggest that KIF20A is involved in the fission of RAB6-positive vesicles from Golgi membranes and movement of these vesicles along microtubules (Miserey-Lenkei *et al.*, 2017).

Considering that endometriosis is etiologically associated with ovarian cancer, we hypothesize that KIF20A inhibition by BKS0349 could prevent cell proliferation and induce apoptosis in endometriotic lesions, similar to events that KIF20A inhibition causes in cancer cells. If so, BKS0349 could offer a viable therapeutic option for the treatment of endometriosis with lasting impact and minimal side effects. For this purpose, we studied the effect of BKS0349 on the development of endometriotic lesions generated in a xenograft mouse model of endometriosis and determined the effect of BKS0349 on lesion size, proliferation, apoptosis, and angiogenesis *in vivo*.

Material and Methods

Endometrial Tissue Collection

Human biopsies of eutopic endometrial tissue (n=4) at the late proliferative/early secretory phase were obtained from egg donors at the time of an oocyte retrieval procedure. Subsequently, endometrial biopsies were harvested in a maintenance medium (M199; Gibco, USA) containing 10% fetal bovine serum [(v/v) FBS; PAA Laboratories], 1% antibiotic-antimycotic solution [(v/v) Gibco, USA), and 10 mmol/L HEPES buffer solution (PAA Laboratories). This study

was approved by the IVI Valencia Clinical Ethics Committee (1606-FIVI-050-FD) and all participants provided written informed consent.

Adenoviral Transfection of Endometrial Fragments

Endometrial biopsies were cut into approximately 3-mm^3 pieces with a scalpel, placed in 96-well plates (2-3 fragments per well) and transfected with Adenovirus mCherry (Ad-mCherry) as previously described (García-Pascual *et al.*, 2015). Briefly, fragments were incubated with Ad-mCherry ($1 \cdot 10^8$ plaque-forming units (PFU)/mL) diluted in antibiotic-free DMEM F-12 (Life Technologies) and 10% FBS (FBS Gold; PAA) medium overnight (12–18 h) at 37 ºC, with 5% CO_2 inside an incubator with gentle agitation. Tissue fragments were then rinsed with DMEM F12 twice and then replaced with fresh DMEM F12 medium containing 1% antibiotics (streptomycin and penicillin), fungizone (1 mg/mL) (Gibco), and 10% FBS. Fluorescence was observed in the red channel (568 nm) with the use of an inverted microscope (Eclipse; Nikon) and used to select 40–50 endometrial fragments per biopsy with optimal signal for subsequent engraftment.

Generation of an Endometriosis Mouse Model

A total of 24 six-week-old athymic nude female mice (Charles River Laboratories International) were used in this study. Mice were housed in pathogen–free conditions at 26 ºC with a 12-h light–12-h dark cycle and fed *ad libitum*. To avoid cycle-dependent variations, animals were ovariectomized and hormone levels were homogenized by 60-day-release pellets containing 18 mg of 17b-E2 (Innovative Research of America, USA) placed under the neck skin of ovariectomized mice. One week after surgery, four mCherry-labeled human endometrium fragments (each approx. 3 mm^3) were implanted together in the peritoneum of each animal with a n-butyl-ester cyanoacrylate adhesive (3M Animal Care) to form a single endometriotic lesion (Figure 1). To allow for homogeneous distribution of human tissue, each biopsy (n=4) contributed one fragment per mouse to the engraftment. This study was approved by the Institutional Animal Care Committee at the University of Valencia (2017-16), and all

procedures were performed following the guidelines for the care and use of mammals from the National Institutes of Health.

Pharmacologic Interventions

One week after tissue implantation, animals were randomly divided into three groups (n=8 per group): 1) 50 mg/kg/week of Tween20 (vehicle group); 2) 200 mg/kg/week of BKS0349 (experimental group); and 3) 50 µg/kg/day of Cabergoline (Cb2) (positive control group). Vehicle and different drugs were diluted in phosphate-buffered saline (PBS; Sigma-Aldrich, USA). Vehicle and BKS0349 were administered via 100 µL tail vein injections once a week for 4 weeks and Cb2 was orally administrated every day for 21 days (Figure 1). Cb2 was chosen as a positive control based on its effects on endometriosis observed in our previous study (Novella-Maestre *et al.*, 2009). Mouse behavior and weight were monitored daily with no noticeable variation (Figure 1). BKS0349 is a specific KIF20A inhibitor developed and synthesized by Biokinesis (Biokinesis SAS, Paris, France, unpublished data). It is formulated as a nanosuspension at 50 mg/mL in water with 12.5 mg/mL of Tween20.

***In Vivo* Fluorescence Imaging**

Endometriotic lesions generated from mCherry-labeled endometrial tissue implanted into mice were monitored over time using an IVIS Spectrum Preclinical *In Vivo* Imaging System (Perkin-Elmer) and related software coupled to an isoflurane gas anesthesia machine (XG-8 Gas Anesthesia System; Xenogen). Immunofluorescence images were acquired by epiluminescence with a peak absorption/emission pair filter set at 587 nm and 610 nm, respectively. The field of view was set at 10 cm until the maximum intensity was obtained as previously described (García-Pascual *et al.*, 2015). Fluorescence was monitored twice weekly from the first day of treatment (D0) until 72 hours after the end of treatment (D24) (Figure 1).

Quantification of *In Vivo* Fluorescence Images

Images were displayed as false-color photon counts superimposed on a grayscale anatomic image with the optical intensity (photon flux) expressed as the average radiant efficiency in

133 photons/s/cm^2 as previously described (García-Pascual *et al.*, 2015). Regions of interest (ROIs)
134 corresponding to endometriotic lesions were automatically established by the software after
135 manually setting a threshold over the lesion showing minimal intensity. Background
136 fluorescence was automatically calculated and subtracted from the ROI data. Signals from each
137 day were normalized relative to D0 as 100%.

138 **Recovery and Preprocessing of Lesions**

139 After 21 days of treatment, animals were euthanized via CO_2 inhalation, the peritoneal cavity
140 was accessed, and a visual examination was performed. Lesions were recovered and examined
141 macroscopically by scale precision caliper before being fixed in 4% neutral-buffered formalin
142 overnight at 4 ºC, embedded in paraffin, and cut into 3 µm sections for histologic,
143 immunohistochemical, and immunofluorescent characterization or RNA extraction for gene
144 expression analysis. The presence of gland-like structures mimicking human eutopic and
145 ectopic endometrial tissue was confirmed with hematoxylin-eosin staining.

146 **Evaluation of Cellular Proliferation and KIF20A expression**

147 KIF20A expression and cell proliferation were assessed by immunohistochemistry for KIF20A
148 (sc-374508, Santacruz Biotechnologies, USA) and Ki67 (AB9260, Millipore, USA),
149 respectively. DAB staining was performed with an EnVision®+ Dual Link System-HRP
150 (DAB+) Kit (Agilent, CA, USA). Briefly, after deparaffinization, antigen retrieval was
151 performed with citrate buffer at 1 mM, pH 6, at 95 ºC for 10 min and permeabilization was
152 carried out with 1% PBS Normal Goat Serum (NGS) and 0.4% Triton X for 10 min. Slides were
153 then blocked with Dual Endogenous Enzyme Block for 15 min and the primary antibody anti-
154 Ki67 (5 µg/mL) or anti-KIF20A (4 µg/mL) were applied and incubated overnight at 4 ºC.
155 Subsequently, slides were covered with labeled-polymer horse radish peroxidase and incubated
156 for 30 min. Afterward, slides were incubated with 3,3'-diaminobenzidine for 10 min and
157 counterstained with hematoxylin. Samples were visualized and analyzed using a Nikon Eclipse

80 (Japan). Cellular proliferation, visualized by Ki67 expression, was quantitatively assessed with Image ProPlus (Media Cybernetics, USA).

TUNEL Assay

Apoptosis in endometriotic lesions from different experimental groups was evaluated with terminal deoxynucleotidyl transferase-mediated dUTP nick end-labeling (TUNEL) staining using fluorescein-labeled cell marker TMR red *in situ* cell death detection kit (Roche, Switzerland) according to the manufacturer's instructions. Cell nuclei were counterstained with 4′,6-diamidino-2-phenylindole (DAPI, Life Technologies, USA). Samples were visualized and analyzed using fluorescence microscopy ZEISS-Axio Vert. A1 (Germany). Four fluorescence images per endometriotic lesion were quantitatively assessed with Image ProPlus (Media Cybernetics, USA) by analyzing each TUNEL image with its corresponding DAPI image and thereby, TUNEL signal was normalized with its corresponding background.

qRT-PCR Analysis

Total RNA from endometriotic lesions embedded in paraffin was extracted using a RNeasy Formalin-Fixed Paraffin-Embedded (FFPE) mini Kit (Qiagen, Germany) and cDNA was synthesized using a PrimeScript RT Reagent kit (Takara, Japan). *CCND1* gene expression, which is a G1 phase-related gene that provide information about cell cycle status, was measured by quantitative real-time polymerase chain reaction (qRT-PCR) using the following primers: 5'-TGGTGAACAAGCTCAAGTG-3' (forward) and 5'-TTCATTTCCAATCCGCCC-3' (reverse). The reaction was carried out using the StepOnePlus System (Applied Biosystems, CA) and PowerUp SYBR Green (ThermoFisher, MA). Qiagen Data Analysis Software was used to calculate fold regulation using *GAPDH* expression for normalization.

Statistical Analysis

GraphPad Prism 6.0 was used for statistical analyses and graphics generation (San Diego, CA, US). Data are presented as mean ± standard deviation (SD). A Wilcoxon test was performed for ROI analysis from different days between groups, immunohistochemistry of KIF20A and Ki67,

and TUNEL analysis in endometrial lesions. A paired t-test was performed for ROIS analysis from different days within the same group. Gene expression analyses of *CCND1* was carried out with Qiagen Data Analysis Software applying Student's t-test. P value < 0.05 was considered statistically significant.

RESULTS

Assessment of Endometriotic Lesions by Fluorescence Lifetime Imaging

Endometriotic lesion size was determined by *in vivo* monitoring using fluorescence lifetime imaging (Figure 2A). We observed that the intensity of the fluorescent signals from endometriotic fragments in all groups were similar at the beginning of the experiment (D0) and normalized the signals from each day to the signal on D0. After the first week of treatment, a uniform reduction in the fluorescent signal was observed in all groups over time, as expected in accordance with the episomal and transient expression of adenoviral particles. However, this reduction was not pronounced in the control group, in which an increase was observed from day 17 to day 24 (Figure 2B), demonstrating an increase in endometriotic lesion growth. While the fluorescent signal continued to decline in treated groups, showing a significant decrease on D24 in the BKS0349 group (p value = 0.0313) and from D14 on the Cb2 group (p value = 0.0313 on days 14-21; p value = 0.0156 on day 24) compared to D0 (Figure 2C-D). In addition, when the signal intensity was compared between groups at different time points, a significant decrease was observed at 72 hours after the end of treatment (D24) in the BKS0349 group compared to the control group (40 ± 19.3% versus 81 ± 30.7%; mean ± SD n=8, p value = 0.0303) (Figure 2E). Differences in fluorescence intensity between the control and Cb2 groups, although noticeable (52 ± 31.2% versus 81 ± 30.7%; mean ± SD n=8), were not statistically significant at the end of the treatment period (Figure 2E).

Macroscopic and Histological Evaluation of Endometriotic Lesions

Seventy-two hours after the end of treatment, animals were euthanized, and lesions were recovered. Subsequently, lesion size on D24 was measured using a scale precision caliper. We found a statistically significant size reduction in endometriotic lesions in the BKS0349 group (0.073 mm^2 ± 0.022; mean ± SD n=8, *p* value = 0.0006) and in the positive control group (Cb2) (0.074 mm^2 ± 0.042; mean ± SD n=8, *p* value = 0.0260) compared to the control group (0.128 mm^2 ± 0.019; mean ± SD n=8) (Figure 3A-D). Moreover, histological examination of lesions revealed the presence of gland-like structures resembling human endometriotic lesions, confirming that human endometrial fragments were successfully implanted in mice (Figure 3E-G).

Cell Proliferation in Endometriotic Lesions

First, we corroborated that BKS0349 treatment effectively inhibits KIF20A protein in endometriotic lesions generated in our animal model. As expected, immunohistochemical analysis showed a significant reduction of KIF20A protein expression in the BKS0349 group compared to the control group (10 ± 1.4% versus 11 ± 3.5%; mean ± SD n=8, *p* value = 0.0258) and showed a reduction of KIF20A protein in the Cb2 group compared to controls 9 ± 1.6% versus 11 ± 3.5%; mean ± SD n=8, *p* value = 0.004, respectively) (Figure 4A-D). These results indicate that BKS0349 effectively inhibits KIF20A protein expression in endometriotic lesions. Considering that KIF20A regulates cell proliferation due to its important role in cytokinesis, suppression of KIF20A could inhibit cell proliferation and thereby endometriotic lesion growth. For this reason, we assessed cell proliferation in the generated lesions from different animal groups by Ki67 immunohistochemistry and observed a significant reduction in proliferating cells in the BKS0349 group compared to the control group (4 ± 3.4% versus 9 ± 3.8%; mean ± SD n=8, *p* value = 0.0082) (Figure 4E-H) that was even more pronounced than in the positive control group (Cb2) (6 ± 5.8%; mean ± SD n=8). Finally, to assess whether *KIF20A* inhibition can cause cell cycle arrest in the G0/G1 phase, we analyzed expression of *CCND1,* a G1 phase-related gene. We observed that KIF20A inhibition significantly decreased *CCND1* expression in

the BKS0349 group compared to the control group (Fold change = 0.2594; p value = 0.049) (Figure 4I).

Apoptosis in Endometriotic Lesions

A TUNEL assay was used to determine whether KIF20A inhibition can increase apoptosis in the endometriotic lesions in our animal model. Endometriotic lesions in the control group were practically devoid of apoptotic cells (25 ± 13.3%; mean ± SD n=8) (Figure 5A, D, G), while a statistical significant increase in apoptotic cells was observed in endometriotic lesions in the BKS0349 group (40 ± 23.0%) (Figure 5B, E, H, J). We also found an increase in apoptotic cells in the Cb2 group (38 ± 24.9%) (Figure 5C, F, I, J), although this increment was not significant.

Discussion

Accumulating evidence suggests that overexpression of KIF20A may confer a malignant phenotype to certain tumors (Kikuchi *et al.*, 2003; Claerhout *et al.*, 2011; Imai *et al.*, 2011; Ho *et al.*, 2012; Shi *et al.*, 2016; Zhao *et al.*, 2018), including ovarian tumors (Li *et al.*, 2018), by promoting cell proliferation and inhibiting apoptosis. *KIF20A* downregulation inhibits cell proliferation and invasion, induces cell cycle arrest, and promotes apoptosis (Wang *et al.*, 2017). Several studies have reported that endometriosis exhibits immunohistological and molecular alterations similar to those observed in ovarian tumors (Komiyama *et al.*, 2018). However, no data are currently available regarding the role of *KIF20A* in endometriosis. This study describes for the first time the effect of KIF20A inhibition by a KIF20A-specific higher-affinity inhibitor derived from Paprotrain (Tcherniuk *et al.*, 2010; Labrière *et al.*, 2016), BKS0349, in endometriotic lesion development and highlights the possible role of KIF20A in the pathophysiology responsible for the establishment, development, and course of endometriosis.

In vivo monitoring of endometriotic lesions generated in our xenograft animal model showed a significant decrease in these lesions after BKS0349 treatment as well as controls. These findings suggest that KIF20A inhibition by BKS0349 leads to a significant reduction in endometriotic lesion size. In addition, macroscopic examination of endometriotic lesions after different treatments demonstrated that KIF20A inhibition by BKS0349 reduced endometriotic lesion size compared to the control group, even more than our positive control (Cb2), whose efficiency in decreasing endometriotic lesion size was previously described by our group (Novella-Maestre *et al.*, 2009; Delgado-Rosas *et al.*, 2011). These findings suggest that *KIF20A* inhibition produces the same significant size reduction in endometriotic lesions as occurs in cancers in which KIF20A downregulation significantly inhibits tumor development (Taniuchi *et al.*, 2005; Wang *et al.*, 2017; Zhao *et al.*, 2018).

After *in vivo* evaluation, we corroborated in the endometriotic lesions generated that BKS0349 inhibited KIF20A expression. Surprisingly, we observed an inhibitory effect of Cabergoline on KIF20A that had never been described in endometriosis. This unexpected finding could bring a greater understanding about the mechanisms involved in the reduction of endometriotic lesions induced by dopamine agonists previously reported (Novella-Maestre et al., 2009). However, it is premature to conclude that dopamine agonists inhibit cytokine expression based on our results and further investigations should be performed to confirm the possible inhibitory effect of Cabergoline on cytokines expression.

Several cancer studies have suggested that the decrease in tumor growth induced by KIF20A downregulation could be due to the alteration of cell cycle regulation (Yan *et al.*, 2012; Pishas *et al.*, 2015; Wang *et al.*, 2017; Youns and Abdel Halim Hegazy, 2017; Zhao *et al.*, 2018), which affects cell proliferation, cell division and invasion (Wang *et al.*, 2017). Therefore, we focused on cell proliferation in the endometriotic lesions generated in mice subjected to BKS0349 treatment compared to no treatment or to Cb2 treatment, which has proven efficacy in endometriotic lesion size reduction (Novella-Maestre *et al.*, 2009). We demonstrated that *KIF20A* inhibition by BKS0349 significantly decreased cell proliferation in endometriotic

lesions generated, even more than Cb2 treatment, whose inhibitory effect on cell proliferation was previously demonstrated (Novella-Maestre *et al.*, 2009), although this time was not statistically significant. In addition, KIF20A inhibition is reported to suppress expression of cell cycle genes, including cyclins (*CCND1, CCNE1, TP21, and TP27),* and thereby, induces cell cycle arrest in the G0/G1 phase and suppresses the cell cycle transition from the G0/G1 phase to the S phase, inhibiting cell proliferation (Zhao *et al.*, 2018).

Cyclins function as regulators of the cell cycle. CCND1 forms a complex that functions as a regulatory subunit of cyclin-dependent kinase 4 (CDK4), or CDK6, whose activity is required for the G1/S transition (Lamb *et al.*, 2003). To determine whether KIF20A inhibition can cause a cell cycle arrest in the G0/G1 phase, we assessed the expression of *CCND1* in the endometriotic lesions generated in our mouse model. We observed that *CCND1* expression was significantly decreased following BKS0349-mediated inhibition of KIF20A, suggesting that KIF20A inhibition appears to cause a cell cycle arrest at the G0/G1 phase in the endometriotic lesion, which consequently inhibits cell proliferation to reduce endometriotic lesion growth.

Several *in vitro* and *in vivo* studies have demonstrated that the inhibition of KIF20A contributes to cell apoptosis induction in cancer cells (Saito *et al.*, 2017; Geng *et al.*, 2018; Kawai *et al.*, 2018). We found the same trend in our study, increasing the apoptosis rate in endometriotic lesions from animals treated with BKS0349 compared to controls. These findings also support previous studies in which apoptosis induction was demonstrated in cancer cells with KIF20A expression inhibited (Yan *et al.*, 2012; Pishas *et al.*, 2015; Saito *et al.*, 2017; Youns and Abdel Halim Hegazy, 2017; Geng *et al.*, 2018; Kawai *et al.*, 2018).

In conclusion, data from the current study suggests that KIF20A inhibition by BKS0349 induces apoptosis and inhibits cell proliferation by cell cycle arrest at the G0/G1 phase and consequently reduces endometriotic lesion size in a xenograft mouse model of endometriosis. These findings imply that KIF20A expression could be an independent prognostic biomarker for endometriosis and may be useful as a novel therapeutic target for treating endometriosis due to its important role in cell cycle regulation and apoptosis. In this context, due to the suggested relevance of

316 KIF20A expression in endometriosis development, more extensive research of KIF20A
317 expression levels in different types of endometrial tissues and functional studies such as
318 KIF20A inhibition on proliferation, migration invasion and related mechanisms in endometrial
319 cells would be required. In addition, further studies to determine the mechanism through which
320 BKS0349 reduces cell proliferation and induces apoptosis in endometriotic lesions, as well as
321 analyze the effects observed in these lesions in other tissues would be necessary before clinical
322 translation to humans.

323

324 **Acknowledgements**

325 The authors express their sincere thanks to the veterinary staff at the Centro de Investigación
326 Principe Felipe (CIPF) animal facilities for their help and collaboration on surgical interventions
327 and animal care. In addition, the authors thank the study participants and the medical staff at the
328 IVI-RMA Valencia clinics for their assistance in obtaining the samples.

329

330 **Authors' roles**

331 H.F. was involved in study design, executed experiments, and wrote and edited the
332 manuscript. A.C. was involved in experimental execution and wrote the manuscript.
333 A.Q. were involved in animal model development as well as functional analysis. C.B.
334 and P.P. gently provided BKS0349 and edited the manuscript. A.P. devised and
335 supervised the study, contributed to data interpretation, and drafted the manuscript. F.D.
336 coordinated the study design, contributed to data interpretation, and edited the
337 manuscript. All authors reviewed the manuscript and provided critical feedback and
338 discussion.

339

340

Study Funding

This research was funded by Biokinesis and supported by the IVI Foundation and the Spanish Ministry of Economy and Competitiveness through the Miguel Servet Program (CPII018/00002) awarded to F.D. and the Sara Borrell Program (CD15/00057) awarded to H.F. Additional funding was provided by the VALi+d Programe (Generalitat Valenciana; ACIF/2016/444) awarded to A.C.

Conflict of interest

The authors have no conflicts of interest to declare.

References

Anglesio MS, Yong PJ. Endometriosis-associated Ovarian Cancers. *Clin Obstet Gynecol* 2017;**60**:711–727.

Barreta A, Sarian LO, Ferracini AC, Costa LBE, Mazzola PG, Angelo Andrade L de, Derchain S. Immunohistochemistry expression of targeted therapies biomarkers in ovarian clear cell and endometrioid carcinomas (type I) and endometriosis. *Hum Pathol* 2019; 85:72-81 .

Claerhout S, Lim JY, Choi W, Park Y-Y, Kim K, Kim S-B, Lee J-S, Mills GB, Cho JY. Gene expression signature analysis identifies vorinostat as a candidate therapy for gastric cancer. In McCormick DL, editor. *PLoS One* 2011;**6**:e24662.

Delgado-Rosas F, Gómez R, Ferrero H, Gaytan F, Garcia-Velasco J, Simón C, Pellicer A. The effects of ergot and non-ergot-derived dopamine agonists in an experimental mouse model of endometriosis. *REPRODUCTION* 2011;**142**:745–755.

Echard A, Jollivet F, Martinez O, Lacapère JJ, Rousselet A, Janoueix-Lerosey I, Goud B. Interaction of a Golgi-associated kinesin-like protein with Rab6. *Science* 1998;**279**:580–585.

García-Pascual CM, Martínez J, Calvo P, Ferrero H, Villanueva A, Pozuelo-Rubio M, Soengas M, Tormo D, Simón C, Pellicer A, *et al.* Evaluation of the potential therapeutic effects of a double-stranded RNA mimic complexed with polycations in an experimental mouse model of endometriosis. *Fertil Steril* 2015;**104**:1310–1318.

Geng A, Qiu R, Murai K, Liu J, Wu X, Zhang H, Farhoodi H, Duong N, Jiang M, Yee J, *et al.* KIF20A/MKLP2 regulates the division modes of neural progenitor cells during cortical development. *Nat Commun* 2018;**9**:2707.

Giudice LC. Clinical practice. Endometriosis. *N Engl J Med* 2010;**362**:2389–2398.

Giudice LC, Kao LC. Endometriosis. *Lancet (London, England)* 2004;**364**:1789–1799.

Ho JR, Chapeaublanc E, Kirkwood L, Nicolle R, Benhamou S, Lebret T, Allory Y, Southgate J,

Radvanyi F, Goud B. Deregulation of Rab and Rab effector genes in bladder cancer. In Hong W, editor. *PLoS One* 2012;**7**:e39469.

Imai K, Hirata S, Irie A, Senju S, Ikuta Y, Yokomine K, Harao M, Inoue M, Tomita Y, Tsunoda T, *et al.* Identification of HLA-A2-restricted CTL epitopes of a novel tumour-associated antigen, KIF20A, overexpressed in pancreatic cancer. *Br J Cancer* 2011;**104**:300–307.

Kajiyama H, Suzuki S, Yoshihara M, Tamauchi S, Yoshikawa N, Niimi K, Shibata K, Kikkawa F. Endometriosis and cancer. *Free Radic Biol Med* 2019;**133**:186–192.

Kawai Y, Shibata K, Sakata J, Suzuki S, Utsumi F, Niimi K, Sekiya R, Senga T, Kikkawa F, Kajiyama H. KIF20A expression as a prognostic indicator and its possible involvement in the proliferation of ovarian clear-cell carcinoma cells. *Oncol Rep* 2018;**40**:195–205.

Kennedy S, Bergqvist A, Chapron C, D'Hooghe T, Dunselman G, Greb R, Hummelshoj L, Prentice A, Saridogan E, ESHRE Special Interest Group for Endometriosis and Endometrium Guideline Development Group. ESHRE guideline for the diagnosis and treatment of endometriosis. *Hum Reprod* 2005;**20**:2698–2704.

Kikuchi T, Daigo Y, Katagiri T, Tsunoda T, Okada K, Kakiuchi S, Zembutsu H, Furukawa Y, Kawamura M, Kobayashi K, *et al.* Expression profiles of non-small cell lung cancers on cDNA microarrays: identification of genes for prediction of lymph-node metastasis and sensitivity to anti-cancer drugs. *Oncogene* 2003;**22**:2192–2205.

Komiyama S, Nagashima M, Taniguchi T, Yokouchi Y, Kugimiya T. Ovarian Clear Cell Carcinoma Detected During Long-Term Management of Endometriotic Cysts in Young Patients: Possible Heterogeneity of this Tumor. *Gynecol Obstet Invest* 2019; 84(3):305-312.

Küpker W, Felberbaum RE, Krapp M, Schill T, Malik E, Diedrich K. Use of GnRH antagonists in the treatment of endometriosis. *Reprod Biomed Online* 2002; **5**:12–16.

Labrière C, Talapatra SK, Thoret S, Bougeret C, Kozielski F, Guillou C. New MKLP-2

inhibitors in the paprotrain series: Design, synthesis and biological evaluations. *Bioorg Med Chem* 2016;**24**:721–734.

Lamb J, Ramaswamy S, Ford HL, Contreras B, Martinez R V, Kittrell FS, Zahnow CA, Patterson N, Golub TR, Ewen ME. A mechanism of cyclin D1 action encoded in the patterns of gene expression in human cancer. *Cell* 2003;**114**:323–334.

Li H, Zhang W, Sun X, Chen J, Li Y, Niu C, Xu B, Zhang Y. Overexpression of kinesin family member 20A is associated with unfavorable clinical outcome and tumor progression in epithelial ovarian cancer. *Cancer Manag Res* 2018;**10**:3433–3450.

Miserey-Lenkei S, Bousquet H, Pylypenko O, Bardin S, Dimitrov A, Bressanelli G, Bonifay R, Fraisier V, Guillou C, Bougeret C, *et al.* Coupling fission and exit of RAB6 vesicles at Golgi hotspots through kinesin-myosin interactions. *Nat Commun* 2017;**8**:1254.

Morita H, Matsuoka A, Kida J-I, Tabata H, Tohyama K, Tohyama Y. KIF20A, highly expressed in immature hematopoietic cells, supports the growth of HL60 cell line. *Int J Hematol* 2018;**108**:607–614.

Novella-Maestre E, Carda C, Noguera I, Ruiz-Saurí A, García-Velasco JA, Simón C, Pellicer A. Dopamine agonist administration causes a reduction in endometrial implants through modulation of angiogenesis in experimentally induced endometriosis. *Hum Reprod* 2009;**24**:1025–1035.

Pishas KI, Adwal A, Neuhaus SJ, Clayer MT, Farshid G, Staudacher AH, Callen DF. XI-006 induces potent p53-independent apoptosis in Ewing sarcoma. *Sci Rep* 2015;**5**:11465.

Practice Committee of the American Society for Reproductive Medicine. Endometriosis and infertility. *Fertil Steril* 2004;**81**:1441–1446.

Saito K, Ohta S, Kawakami Y, Yoshida K, Toda M. Functional analysis of KIF20A, a potential immunotherapeutic target for glioma. *J Neurooncol* 2017;**132**:63–74.

Sayasneh A, Tsivos D, Crawford R. Endometriosis and ovarian cancer: a systematic review.

ISRN Obstet Gynecol 2011;**2011**:140310.

Shi C, Huang D, Lu N, Chen D, Zhang M, Yan Y, Deng L, Lu Q, Lu H, Luo S. Aberrantly activated Gli2-KIF20A axis is crucial for growth of hepatocellular carcinoma and predicts poor prognosis. *Oncotarget* 2016;**7**:26206–26219.

Somigliana E, Vigano' P, Parazzini F, Stoppelli S, Giambattista E, Vercellini P. Association between endometriosis and cancer: a comprehensive review and a critical analysis of clinical and epidemiological evidence. *Gynecol Oncol* 2006;**101**:331–341.

Taniuchi K, Nakagawa H, Nakamura T, Eguchi H, Ohigashi H, Ishikawa O, Katagiri T, Nakamura Y. Down-regulation of RAB6KIFL/KIF20A, a kinesin involved with membrane trafficking of discs large homologue 5, can attenuate growth of pancreatic cancer cell. *Cancer Res* 2005;**65**:105–112.

Tcherniuk S, Skoufias DA, Labriere C, Rath O, Gueritte F, Guillou C, Kozielski F. Relocation of Aurora B and survivin from centromeres to the central spindle impaired by a kinesin-specific MKLP-2 inhibitor. *Angew Chem Int Ed Engl* 2010;**49**:8228–8231.

Verhey KJ, Hammond JW. Traffic control: regulation of kinesin motors. *Nat Rev Mol Cell Biol* 2009;**10**:765–777.

Wang M, Liu K, Zhou X-L, Mei S-Y, Zhang C-J, Zhang T-G. *Downregulation of KIF20A induces cell cycle arrest and apoptosis by suppressing PI3K/AKT in human glioblastoma*. *Int J Clin Exp Med* 2017;**10**:.

Yan G-R, Zou F-Y, Dang B-L, Zhang Y, Yu G, Liu X, He Q-Y. Genistein-induced mitotic arrest of gastric cancer cells by downregulating KIF20A, a proteomics study. *Proteomics* 2012;**12**:2391–2399.

Youns M, Abdel Halim Hegazy W. The Natural Flavonoid Fisetin Inhibits Cellular Proliferation of Hepatic, Colorectal, and Pancreatic Cancer Cells through Modulation of Multiple Signaling Pathways. In Ahmad A, editor. *PLoS One* 2017;**12**:e0169335.

Zafrakas M, Grimbizis G, Timologou A, Tarlatzis BC. Endometriosis and Ovarian Cancer Risk: A Systematic Review of Epidemiological Studies. *Front Surg* 2014;**1**:14.

Zhao X, Zhou L-L, Li X, Ni J, Chen P, Ma R, Wu J, Feng J. Overexpression of KIF20A confers malignant phenotype of lung adenocarcinoma by promoting cell proliferation and inhibiting apoptosis. *Cancer Med* 2018;**7**:4678–4689.

Figure Legends

FIGURE 1. Experimental design of endometriosis mouse model. Six-week-old athymic nude female mice were ovariectomized and implanted with 60-day E2-release pellets. Subsequently, mCherry-labeled human endometrium fragments were implanted in the peritoneum of each animal. One week after tissue implantation, mice were divided into three treatment groups (n=8/group). Vehicle and BKS0349 were given by tail vein injection once a week, and Cabergoline (Cb2) was orally administered every day for 21 days. mCherry-labeled endometriotic lesions were monitored twice weekly from the start of treatment (D0) until 72 hours after the treatment stopped (D24) using an IVIS Spectrum Preclinical *In Vivo* Imaging System. After 21 days of treatment, mice were euthanized, and lesions were recovered.

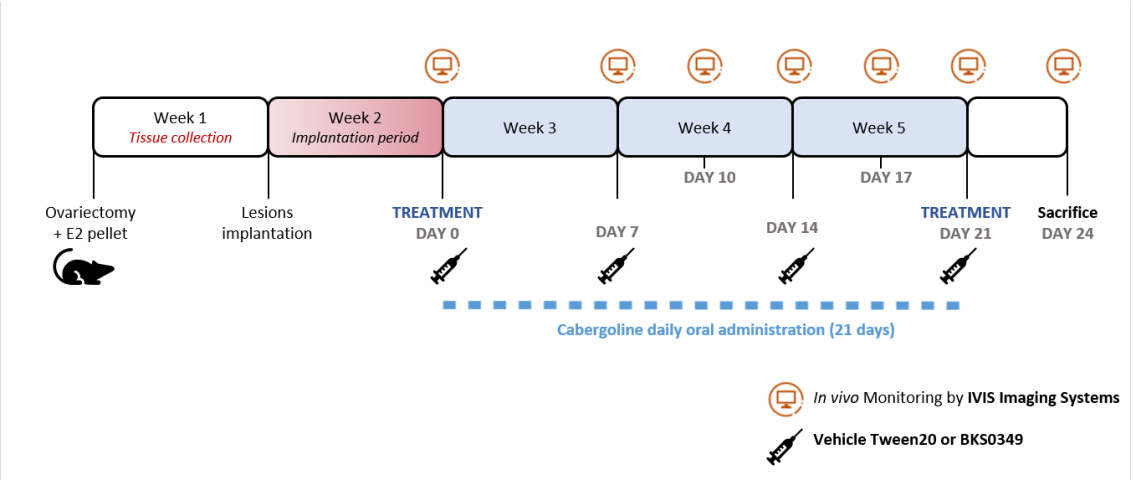

FIGURE 2. *In vivo* monitoring of endometriotic lesions. Examples of the fluorescent signaling provided by mCherry-labeled endometriotic implants in control, BKS0349, and Cabergoline (Cb2) treated animals (n=8/group) (A). Quantitative analysis of mean ± SD fluorescence intensity provided by lesions generated in the control group (B), BKS0349 group (C), and the Cb2 group (D) from day0 (D0) to D24 and in the three groups (E). Fluorescence intensity was expressed as the photon flux (photons/s) and normalized to the value on D0. * *p* value < 0.05; ** *p* value 0.01 compared to D0 (B,C,D) or control (E).

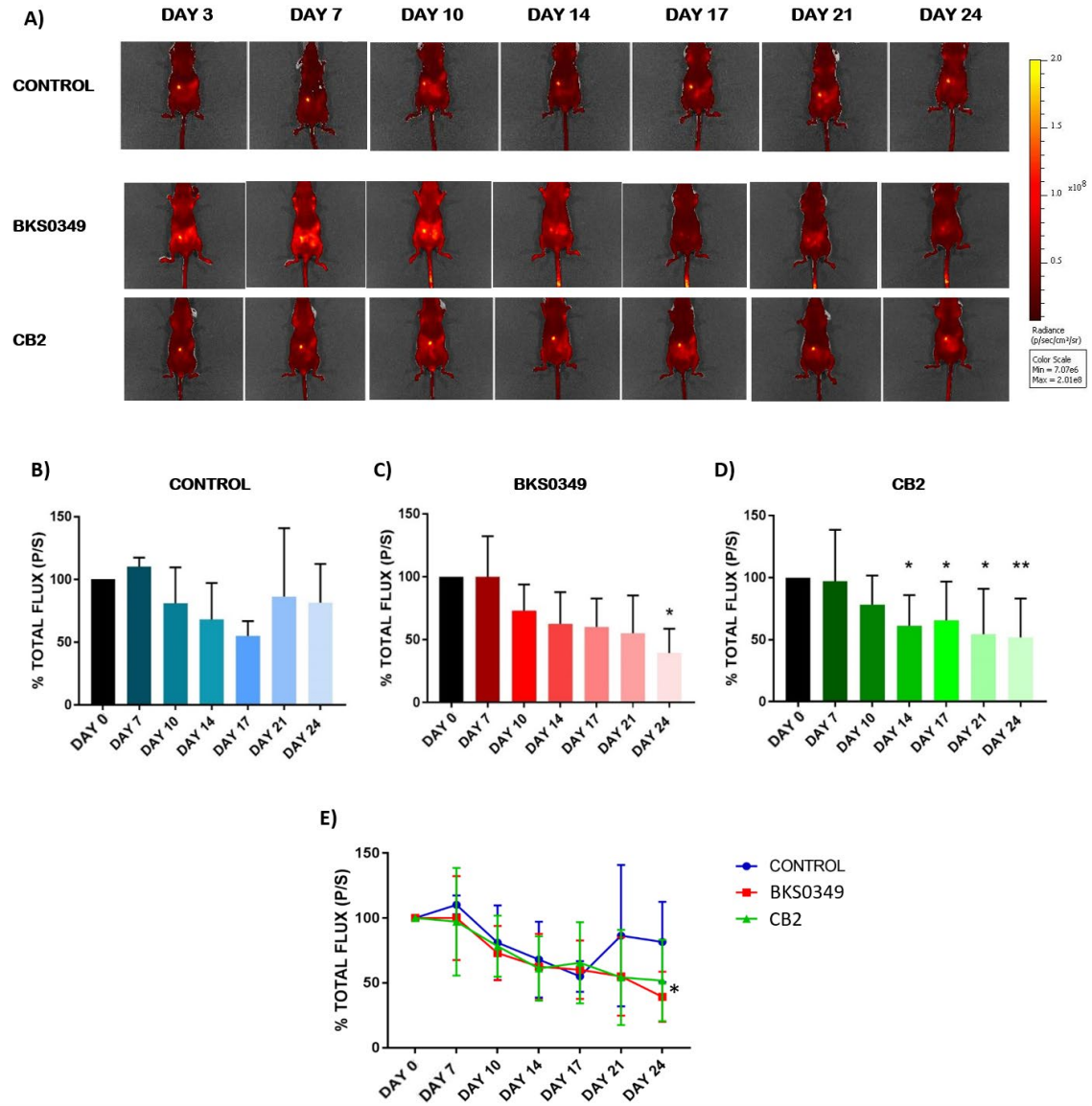

FIGURE 3. Effect of BKS0349 on macroscopic and histologic features of endometriotic lesions. Macroscopic observations and histologic evaluation of endometriotic lesions generated in vehicle-treated control (A, E), BKS0349-treated (B, F), and Cb2-treated (C, G) mice at the end of the 21-day treatment period (n=8/group). Lesion size is represented in mm^2. Black scale bars = 5 mm and white scale bars = 50 µm. * $p < 0.05$; ** $p < 0.01$.

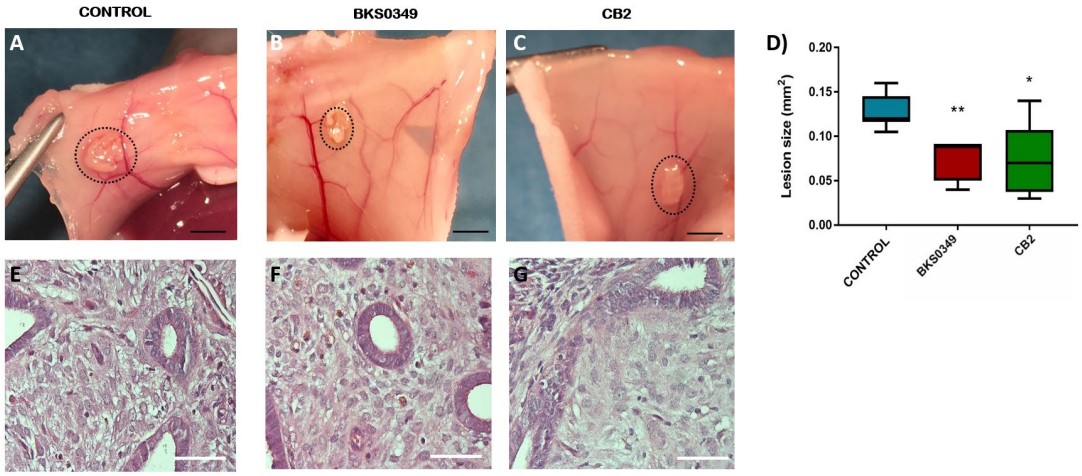

FIGURE 4. Effect of BKS0349 on cell cycle and cell proliferation in endometriotic lesions. Immunohistochemical staining of KIF20A protein in control (A), BKS0349 (B), and Cb2 (C) groups. Quantitative analysis of the percentage of KIF20A protein expression in the different groups (D), expressed as mean ± SD. Immunohistochemical staining of Ki67 (proliferation marker) in control (E), BKS0349 (F), and Cb2 (G) groups. Quantitative analysis of the percentage of Ki67-positive cells in the different groups (H) expressed as mean ± SD. *CCND1* gene expression in each group (I) expressed as fold change. Red arrow shows example of positive staining. Scale bars = 50 µm. *$p < 0.05$.

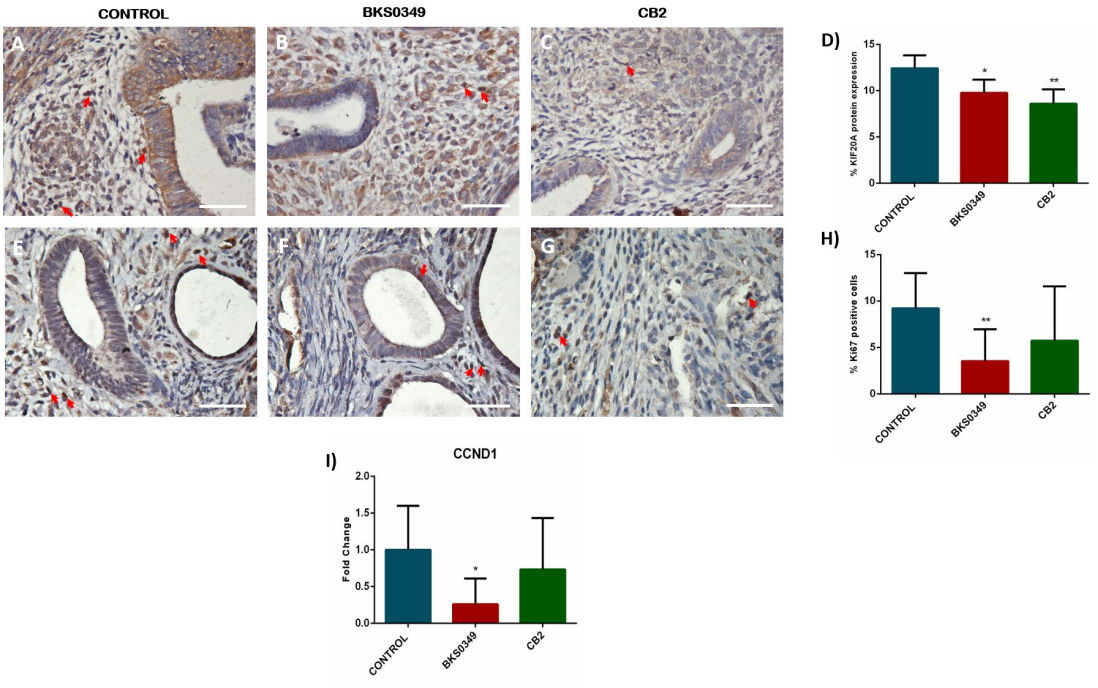

FIGURE 5. Effect of BKS0349 on apoptosis in endometriotic lesions. Analysis of apoptosis by TUNEL staining in endometriotic lesions from different treatment groups. DAPI nuclear staining (blue) was used to stain nuclei (A, B, C). Apoptotic cells were identified by labeling DNA breaks induced by DNAse I (red color) (D, E, F). Merge of TUNEL images in control (G), BKS0349 (H), and Cb2 (I) treatment groups. Quantitative analysis of the percentage of apoptotic cells in the different groups (J). Data are expressed as mean ± SD. Scale bars = 50 µm. * $p < 0.05$.